e-ISSN 2320 –7876 www.ijfans.org
Vol.11, Iss.9, Dec 2022

Research Paper

Structural and magnetic properties of nickel-cobalt spinel ferrite nanoparticles synthesized by simple combustion method

G. Veeramani [1,*], S. Peter Vijay [1], G. Padma Priya[1]
[1] Department of Chemistry, Faculty of Arts and Science,
Bharath Institute of Higher Education and Research (BIHER),
Chennai – 600073, Tamil Nadu, India
***Corresponding Author Email addresses: veeramani@gmail.com (G. Veeramani)**

Address for Correspondence

G. Veeramani [1,*], S. Peter Vijay [1], G. Padma Priya[1]
[1] Department of Chemistry, Faculty of Arts and Science,
Bharath Institute of Higher Education and Research (BIHER),
Chennai – 600073, Tamil Nadu, India
***Corresponding Author Email addresses: veeramani@gmail.com (G. Veeramani)**

Abstract

Spinel Ni-Co ferrite nanoparticles were prepared by simple combustion method and investigated through XRD, SEM, TEM and SAED analyses. Powder XRD and SAED data indicated the presence of nanocrystalline cubic spinel with single phase. The lattice parameters of the samples gradually increased with increasing Ni concentration and follow Vegard's law. The crystallite size (D) and X-ray density of Ni-Co ferrite samples decreased with increasing Ni concentration. The spherical shape morphology of spinel Ni-Co ferrite particles and grain size (22.42, 21.32 and 20.62 nm for x = 0.0, 0.3 and 0. 5, respectively) was established by TEM. VSM analysis showed the typical magnetic properties of Ni-Co ferrite. The shape of the magnetic hysteresis (M-H) loops revealed the dependence of superparamagnetic behavior at room temperature (RT).

Keywords: Spinel Ni-Co ferrite; Sol-gel combustion; Nanoparticles; paramagnetic behavior.

1. Introduction

In general, high remanent magnetization (Mr) and high coercivity (Hc) indicates hard ferrites, which are often used to make permanent magnets, whereas soft ferrites with slim hysteresis loop, ensuing in almost zero Mr and very low Hc, are used for magnetic shielding, sensors, transformers, magnetic recording, photomagnetic and microwave devices [1-5].

Recently, nano sized iron based magnetic ferrite nanocatalyst with the general formula AB_2O_4 have been showing extra ordinary properties, due to their, high coercivity, moderate magnetization and single domain, which have various applications in technological, biological and industrial fields [6-10]. The enhancement of Ms can be limited by structural changes in related to the instantaneous localization of Co ions in the A- and B- sites of the spinel Ni-Costructure in relation with the synthesis method, sintering temperature, processing conditions, morphology and grain size [11].

Among them, $CoFe_2O_4$ has a inverse spinel structure (Co ions occupy A- sites and half of Fe^{3+} ions occupy A- and B- sites, respectively) and the replacement of higher-magnetic Co ions by the Ni ions ions enhanced the magnetization in the Ni-Co system. Generally, spinel Ni-Co samples are soft magnetic nano- ferrites with excellent catalytic activity, chemical stability and high electrical resistivity [11-14]. The type of starting precursors, substitution of cations and their distribution among both interstitial sites (A- and B- sites) in spinel system can be attuned, ensuing in diverse magnetic properties. In the last few years, spinel ferrite nanoparticles have been prepared using various methods, such as sol-gel, co-precipitation, ball-milling, microemulsions, polyol, hydrothermal-solvothermal, and microwave composition methods, etc. [15-18]. In spinel ferrites, the magnetic properties are affected by the presence of disordered spins and the cations distribution in the A- and B- sites on spinel surfaces. It is well known that the synthesis route influence the physico-chemical, optical, electrical, magnetic and catalytic properties of ferrites. The magnetic nature of nanoparticles has strong inclination to aggregate resulting in a different magnetic comportment comparing to non-magnetic metal oxide nanoparticles [19]. In this present work, we have investigated the effect of synthesis method and Ni concentration on the structural, morphological and magnetic behavior of Ni-Co (x = 0.0, 0.3 and 0.5) NPs.

2. Experimental part

Ni-Co ferrite (x = 0.0, 0.3 and 0.5) NPs were prepared by a modified sol-gel route by mixing ferric nitrate ($Fe(NO_3)_3{\cdot}9H_2O$), nickel nitrate ($Ni(NO_3)_3.6H_2O$) and cobalt nitrate ($Co(NO_3)_2{\cdot}6H_2O$) with urea (N_2H_4CO), under continuous stirring, for 30 min. All chemicals by this synthesis route were used without additional purification. In this study, urea was used as the fuel and reducing agent. The precursors and the dopant were together dissolved in a minimum

amount of urea solution and stirred for 10 minutes on a magnetic stirrer at room temperature (RT) until a homogenous mixture was obtained. The mixture was then heated in an electric oven for about 1 hour at 70°C until a dry gel was formed. The gel so formed was annealed in air furnace at 500° C for 3 hours, due to get the final products. The synthesis procedure was repeated by taking different proportions of cobalt and nickel for doped samples.

3. Results and discussion

Powder XRD patterns shows the evolution of spinel phase with the increase of Ni concentration in Ni-Co (x = 0.0, 0.3 and 0.5) system (Fig. 1). The crystallization degree decreases with increasing Ni concentration; which indicated the lower intense and sharp diffraction lines are remarked. No extra reflections are observed, indicating the synthesis of pure, well-crystallized spinel ferrite. In all samples, the most intense lines are attributed single phase, with Miller indices (111), (220), (311), (222), (400), (422), (511), (440) crystallizing in cubic spinel structure with space group *Fd-3m* [20,21]. For x = 0.0, 0.3 and 0.5, spinel $CoFe_2O_4$ (JCPDS card 16-6202) main phase were observed.

The D value decrease from 26.45 nm to 22.65 nm at x = 0.0 to 0.5, also suggested by the highly crystallized ferrite from XRD pattern. The increase of Ni concentration reduces the intensity of diffraction peaks comparing to $CoFe_2O_4$ [22].

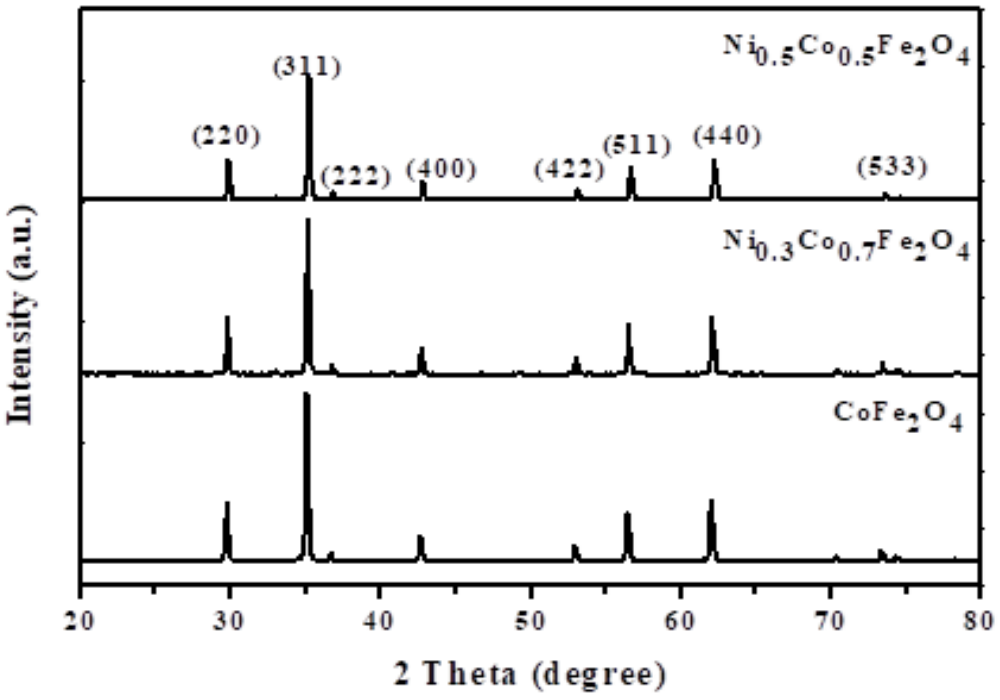

e-ISSN 2320 –7876 www.ijfans.org
Vol.11, Iss.9, Dec 2022

Figure 1. Powder XRD patterns of spinel Ni-Co ferrite (x = 0.0, 0.3 and 0.5) NPs.

The lattice constant of Ni-Co system shows a decreasing trend with increasing Ni concentration, from 8.304 Å (x = 0.0) to 8.295 Å (x = 0.5), and could be attributed to the substitution of larger ionic radius Co ions (0.72 Å) by smaller ionic radius Ni ions (0.69 Å) [23]. By the substitution of Co ions with Ni ions in the Ni-Cosystem, Ni ions starts to occupy the A-sites and Fe^{3+} migrates from A to B- sites, displacing Co ions. By increasing the number of Fe^{3+} in B- sites, the system changes from inverse spinel to normal spinel structure. This process produces a slight shift of peaks in the XRD patterns [24].

The FT-IR spectra of spinel Ni-CoNPs are shown in Figure 2. The band at 520-850 cm^{-1} corresponds to the intrinsic lattice vibration of O–M–O bond in the spinel system [25]. The FT-IR absorption bands at 1620-1655 cm-1 corresponding to bending vibration of H–O–H bond. Band at 3420-3250 cm^{-1} corresponds to the vibration of water molecule in the spinel system [26].

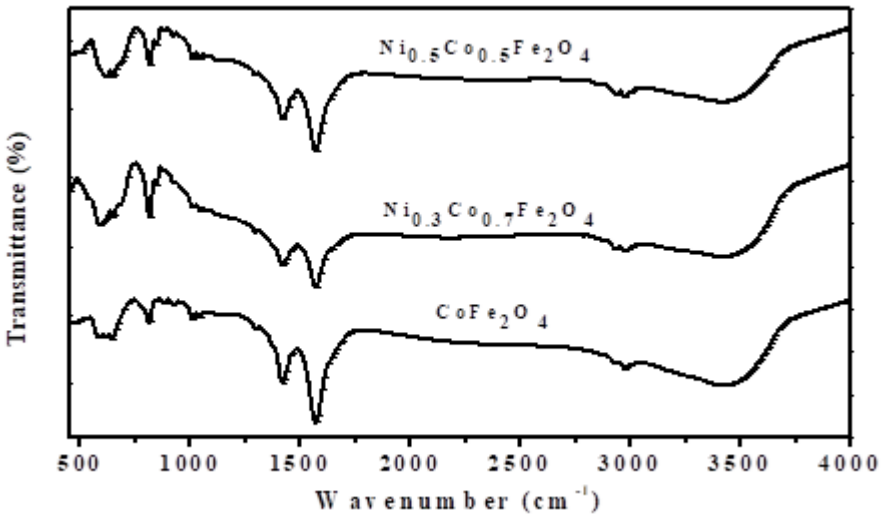

Figure 2. FT-IR spectra of spinel Ni-Co ferrite (x = 0.0, 0.3 and 0.5) NPs.

The surface morphology and shape of Ni-Co ferrite NPs were investigated by SEM analysis (Figure 3). SEM images clearly showed the spherical shaped particles like morphology with less than 40 nm in the grain size. Also, observed the agglomeration of the nanoparticles, due to the magnetic interaction of the particles.

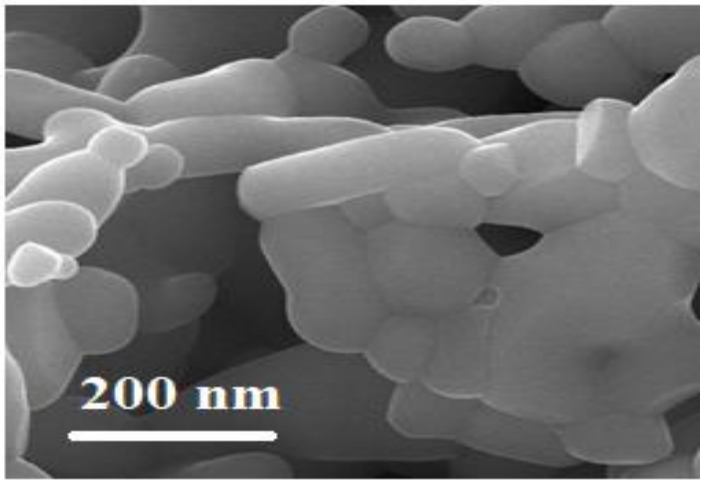

Figure 3. SEM images of spinel $Ni_{0.5}Co_{0.5}Fe_2O_4$ NPs.

Crystal structure and size of Ni-Co ferrite NPs was confirmed by TEM images (Figure 4). The particles size decreasing with the increase of Ni-content, which is similar to the crystallite sizes confirmed by XRD analysis. Also, the nanoparticles appear as agglomerated spherical particles. The spherical shapes of particles may be the result of the synthesis method and surface properties, while the agglomeration may be due to the interfacial surface tension phenomenon.

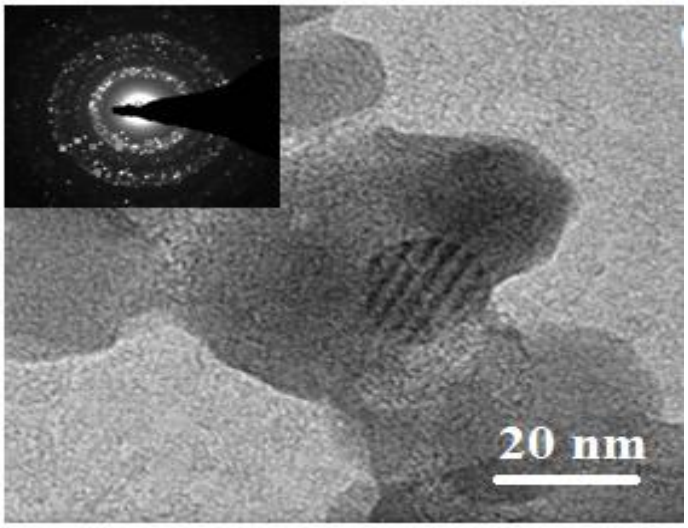

Figure 4. TEM images of spinel $Ni_{0.5}Co_{0.5}Fe_2O_4$ NPs.

The saturation magnetization (MS), remanent magnetization (MR) and coercivity (Hc) are the most significant limitations for a magnetic spinel material, typically, extracted from the

magnetic hysteresis (M-H) loops (Figure 5). Ni-doped $CoFe_2O_4$ NPs (x = 0.5) exhibit a typical M-H loop indicating a superparamagnetic behavior, while the M-H loops of $CoFe_2O_4$ (x = 0.0) and low Ni concentration suggest ferromagnetic behaviors. The sharp peaks suggest higher magnetic purity. The broad peaks, suggest wide distributions of particle sizes and consequently an increased distribution of coercivities (Hc). The increase of Ni ions content makes Fe^{3+} to have less magnetic neighboring ions and the uncoupled rotation of these ions leads to the decrease of MS [27]. The gradually decrease of Ms and MR with increasing Ni concentration, can be explained by the increase of the surface spin canting effect due to increase of Ni concentration. At low Ni ions content, all the Co ions occupy the B-sites, while the Fe^{3+} ions are equally distributed in both A and B sites of the spinel structure [28-31]. By increasing the Ni ions content, it will occupy the B sites forcing a partial migration of Co ions ions to A and of Fe^{3+} ions to B sites, which enhance the magnetic properties of the spinel system.

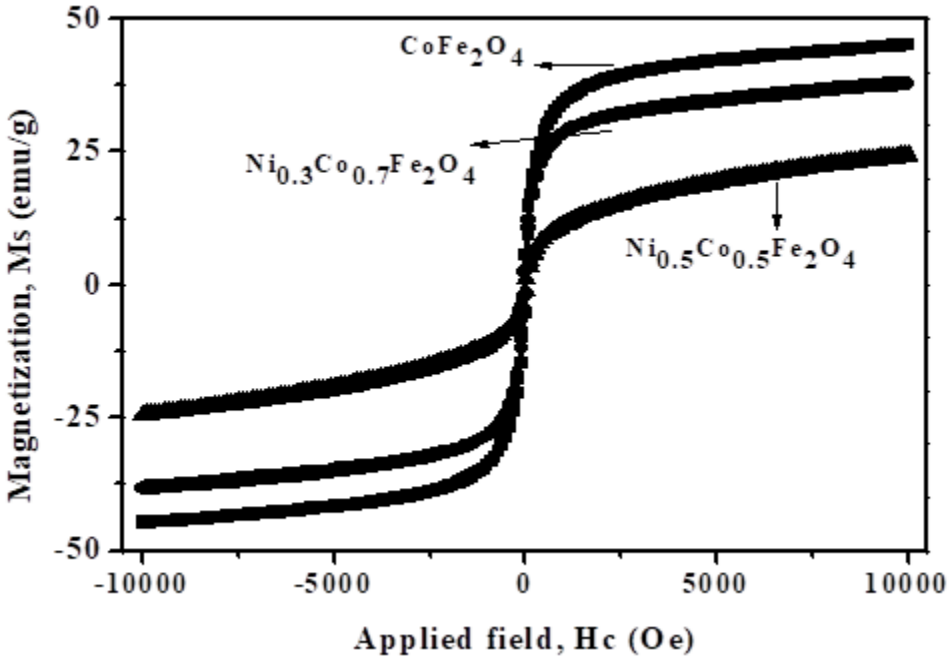

Figure 5. VSM results of spinel Ni-Co ferrite (x = 0.0, 0.3 and 0.5) NPs.

4. Conclusions

Structural, morphology, size, and magnetism of Ni-Co ferrite NPs were investigated. The lattice constant showed decreasing trend with increasing Ni concentration which was attributed to the larger ionic radius of Co ions compared to Ni ions. By increasing the Ni concentration, the

XRD patterns showed pure phase of Ni-Co ferrite NPs. FT-IR spectroscopy confirmed the formation of metal-oxidic phases. SEM and TEM images showed spherical highly agglomerated particles decreasing of grain size with increasing of Ni-content. The magnetic properties are strongly affected by the sample composition and cation distribution within the spinel structure. Ni-doped $CoFe_2O_4$ NPs (x = 0.5) exhibit a typical M-H loop indicating a superparamagnetic behavior, while the M-H loops of $CoFe_2O_4$ (x = 0.0) and low Ni concentration (x = 0.3) suggest ferromagnetic behaviors.

References

1. K. Chinnaraj, A. Manikandan, P. Ramu, S. Arul Antony, P. Neeraja, Comparative study of microwave and sol-gel assisted combustion methods of Fe_3O_4 nanostructures: Structural, morphological, optical, magnetic and catalytic properties, Journal of Superconductivity and Novel Magnetism, 28 (2015) 179-190.
2. E. Hema, A. Manikandan, P.Karthika, M. Durka, S. Arul Antony, B. R. Venkatraman, A novel synthesis of Zn^{2+}-doped $CoFe_2O_4$ spinel nanoparticles: Structural, morphological, opto-magnetic and catalytic properties, Journal of Superconductivity and Novel Magnetism, 28 (2015) 2539-2552.
3. V. Umapathy, A. Manikandan, S. Arul Antony, P. Ramu, P. Neeraja, Synthesis, structural, morphological and opto-magnetic properties of Bi_2MoO_6 nano-photocatalyst by sol-gel method, Transactions of Nonferrous Metals Society of China, 25 (2015) 3271-3278.
4. A. Manikandan, S. Arul Antony, R. Sridhar, Seeram Ramakrishna, M. Bououdina, A simple combustion synthesis and optical studies of magnetic $Zn_{1-x}Ni_xFe_2O_4$ nanostructures for photoelectrochemical applications, Journal of Nanoscience and Nanotechnology, 15 (2015) 4948-4960.
5. A. Manikandan, M. Durka, S. Arul Antony, Magnetically recyclable spinel $Mn_xZn_{1-x}Fe_2O_4$; ($0.0 \leq x \leq 0.5$) nano-photocatalysts, Advanced Science, Engineering and Medicine, 7 (2015) 33-46.
6. A. Manikandan, A. Saravanan, S. Arul Antony, M. Bououdina, One-pot low temperature synthesis and characterization studies of nanocrystalline α-Fe_2O_3 based dye sensitized solar cells, Journal of Nanoscience and Nanotechnology, 15 (2015) 4358-4366.

7. M. F. Valan, A. Manikandan, S. Arul Antony, A novel synthesis and characterization studies of magnetic Co_3O_4 nanoparticles, Journal of Nanoscience and Nanotechnology, 15 (2015) 4580-4586.
8. M. F. Valan, A. Manikandan, S. Arul Antony, Microwave combustion synthesis and characterization studies of magnetic $Zn_{1-x}Cd_xFe_2O_4$ ($0 \leq x \leq 0.5$) nanoparticles, Journal of Nanoscience and Nanotechnology, 15 (2015) 4543-4551.
9. S. Jayasree, A. Manikandan, A. M. Uduman Mohideen, C. Barathiraja, S. Arul Antony, Comparative study of combustion methods, opto-magnetic and catalytic properties of spinel $CoAl_2O_4$ nano- and microstructures, Advanced Science, Engineering and Medicine, 7 (2015) 672-682.
10. A. Mary Jacintha, A. Manikandan, K. Chinnaraj, S. Arul Antony, P. Neeraja, Comparative studies of spinel $MnFe_2O_4$ nanostructures: Structural, morphological, optical, magnetic and catalytic properties, Journal of Nanoscience and Nanotechnology, 15 (2015) 9732-9740. (Impact Factor: 1.354).
11. G. Padmapriya, A. Manikandan, V. Krishnasamy, S. K. Jaganathan, S. Arul Antony, Spinel $Ni_xZn_{1-x}Fe_2O_4$ ($0.0 \leq x \leq 1.0$) nano-photocatalysts: Synthesis, characterization and photocatalytic degradation of methylene blue dye, Journal of Molecular Structure, 1119 (2016) 39-47.
12. G. Mathubala, A. Manikandan, S. Arul Antony and P. Ramar, Photocatalytic degradation of methylene blue dye and magneto-optical studies of magnetically recyclable spinel $Ni_xMn_{1-x}Fe_2O_4$ (x = 0.0-1.0) nanoparticles, Journal of Molecular Structure, 1113 (2016) 79-87.
13. A. Manikandan, M. Durka, S. Arul Antony, Hibiscus rosa-sinensis leaf extracted green methods, magneto-optical and catalytic properties of spinel $CuFe_2O_4$ nano- and microstructures, Journal of Inorganic and Organometallic Polymers and Materials, 25 (2015) 1019–1031.
14. A. Manikandan, M. Durka, K. Seevakan, S. Arul Antony, A novel one-pot combustion synthesis and opto-magnetic properties of magnetically separable spinel $Mn_xMg_{1-x}Fe_2O_4$ ($0.0 \leq x \leq 0.5$) nano-photocatalysts, Journal of Superconductivity and Novel Magnetism, 28 (2015) 1405-1416.

15. A. Manikandan, M. Durka, S. Arul Antony, One-pot flash combustion synthesis, structural, morphological and opto-magnetic properties of spinel $Mn_xCo_{1-x}Al_2O_4$ (x = 0, 0.3 and 0.5) nano-catalysts, Journal of Superconductivity and Novel Magnetism, 28 (2015) 209–218.
16. A. Manikandan, E. Hema, M. Durka, M. Amutha Selvi, T. Alagesan, S. Arul Antony, Mn^{2+} doped NiS ($Mn_xNi_{1-x}S$: x = 0.0, 0.3 and 0.5) nanocrystals: Structural, morphological, opto-magnetic and photocatalytic properties, Journal of Inorganic and Organometallic Polymers and Materials, 25 (2015) 804–815.
17. V. Mary Teresita, A. Manikandan, B. Avila Josephine, S. Sujatha, S. Arul Antony, Electro-magnetic properties and humidity sensing studies of magnetically recoverable $LaMg_xFe_{1-x}O_{3-\delta}$ perovskites nano-photocatalysts by sol-gel route, Journal of Superconductivity and Novel Magnetism, 29 (2016) 1691–1701.
18. S. Jayasree, A. Manikandan, S. Arul Antony, A. M. Uduman Mohideen, C. Barathiraja, Magneto-optical and catalytic properties of recyclable spinel $NiAl_2O_4$ nanostructures using facile combustion methods, Journal of Superconductivity and Novel Magnetism, 29 (2016) 253–263.
19. C. Barathiraja, A. Manikandan, A. M. Uduman Mohideen, S. Jayasree, S. Arul Antony, Magnetically recyclable spinel $Mn_xNi_{1-x}Fe_2O_4$ (x = 0.0–0.5) nano-photocatalysts: Structural, morphological and opto-magnetic properties, Journal of Superconductivity and Novel Magnetism, 29 (2016) 477-486.
20. B. Avila Josephine, A. Manikandan, V. Mary Teresita, S. Arul Antony, Fundamental study of $LaMg_xCr_{1-x}O_{3-\delta}$ perovskites nano-photocatalysts: Sol-gel synthesis, characterization and humidity sensing, The Korean Journal of Chemical Engineering, 33 (2016) 1590-1598.
21. A. Manikandan, M. Durka, M. A. Selvi, S. Arul Antony, Sesamum indicum plant extracted microwave combustion synthesis and opto-magnetic properties of spinel $Mn_xCo_{1-x}Al_2O_4$ nano-catalysts, Journal of Nanoscience and Nanotechnology, 16 (2016) 448-456.
22. A. Manikandan, M. Durka, M. A. Selvi, S. Arul Antony, Aloe vera plant extracted green synthesis, structural and opto-magnetic characterizations of spinel $Co_xZn_{1-x}Al_2O_4$ nano-catalysts, Journal of Nanoscience and Nanotechnology, 16 (2016) 357-373.
23. A. Manikandan, S. Arul Antony, Magnetically separable $Mn_xZn_{1-x}Fe_2O_4$; ($0.0 \leq x \leq 0.5$) nanostructures: Structural, morphological, opto-magnetic and photocatalytic properties,

Synthesis and Reactivity in Inorganic, Metal-Organic, and Nano-Metal Chemistry, 46 (2016) 1277-1297.

24. S. Rajmohan, A. Manikandan, V. Jeseentharani, S. Arul Antony, J. Pragasam, Simple co-precipitation synthesis and characterization studies of $La_{1-x}Ni_xVO_3$ perovskites nanostructures for humidity sensing applications, Journal of Nanoscience and Nanotechnology, 16 (2016) 1650-1655.
25. E. Hema, A. Manikandan, M. Gayathri, M. Durka, S. Arul Antony, B. R. Venkatraman, Role of Mn^{2+}-doping on structural, morphological, optical, magnetic and catalytic properties of spinel $ZnFe_2O_4$ nanoparticles, Journal of Nanoscience and Nanotechnology, 16 (2016) 5929-5943.
26. E. Hema, A. Manikandan, P. Karthika, M. Durka, S. Arul Antony, B. R. Venkatraman, Magneto-optical properties of recyclable spinel $Ni_xMg_{1-x}Fe_2O_4$ ($0.0 \leq x \leq 1.0$) nano-catalysts, J. Nanoscience and Nanotechnology, 16 (2016) 7325-7336.
27. S. Moortheswaran, A. Manikandan, S. Sujatha, S. K. Jaganathan, S. Arul Antony, One-pot combustion synthesis and characterization studies of spinel $CoAl_2O_4$ nano-catalysts, Nanoscience and Nanotechnology Letters, 8 (2016) 424-427.
28. S. Moortheswaran, A. Manikandan, S. Sujatha, S. K. Jaganathan, S. Arul Antony, Selective catalytic oxidation of benzyl alcohol and characterization studies of spinel $MnAl_2O_4$ nanoparticles by a facile synthesis route, Nanoscience and Nanotechnology Letters, 8 (2016) 434-437.
29. P. Thilagavathi, A. Manikandan, S. Sujatha, S. K. Jaganathan, S. Arul Antony, Sol-gel synthesis and characterization studies of $NiMoO_4$ nanostructures for photocatalytic degradation of methylene blue dye, Nanoscience and Nanotechnology Letters, 8 (2016) 438-443.
30. S. Rajmohan, V. Jeseentharani, A. Manikandan, J. Pragasam, Co-precipitation synthesis method, characterizations and humidity sensing applications of perovskite-type mixed oxide $La_{1-x}Co_xVO_{3-\delta}$ nanocomposites, Nanoscience and Nanotechnology Letters, 8 (2016) 393-398.
31. K. Seevakan, A. Manikandan, P. Devendran, S. Arul Antony, T. Alagesan, One-pot synthesis and characterization studies of iron molybdenum mixed metal oxide

($Fe_2(MoO_4)_3$) nano-photocatalysts, Advanced Science, Engineering and Medicine, 8 (2016) 566-572.